

Functional approaches to infrared Yang-Mills theory in the Coulomb gauge

A Weber^{1,*}, M Leder², J M Pawłowski^{3,4} and H Reinhardt²

¹ Instituto de Física y Matemáticas, Universidad Michoacana de San Nicolás de Hidalgo, Edificio C-3, Ciudad Universitaria, 58040 Morelia, Michoacán, Mexico

² Institut für Theoretische Physik, Universität Tübingen, Auf der Morgenstelle 14, 72076 Tübingen, Germany

³ Institut für Theoretische Physik, Universität Heidelberg, Philosophenweg 16, 69120 Heidelberg, Germany

⁴ ExtreMe Matter Institute EMMI, GSI Helmholtzzentrum für Schwerionenforschung, Planckstr. 1, 64291 Darmstadt, Germany

June 10, 2011

Abstract

We present the current status of ongoing efforts to use functional methods, Dyson-Schwinger equations and functional renormalization group equations, for the description of the infrared regime of nonabelian (pure) gauge theories in the Coulomb gauge. In particular, we present a new determination of the color-Coulomb potential with the help of the functional renormalization group that results in an almost linearly rising potential between static color charges at large spatial distances.

*Speaker. Email: axel@ifm.umich.mx

1 Introduction

Important progress has been achieved over the last decade in the description of the deep infrared region of nonabelian gauge theories with the help of functional methods, employing Coulomb gauge fixing. By functional methods we refer to semi-analytical tools that do *not* make use of the discretization of space-time as does lattice gauge theory. Specifically, equations of Dyson-Schwinger type arising from a variational principle have been used, and more recently functional renormalization group equations. In this contribution, we will report on the current status of these investigations. We will focus exclusively on pure gauge theories, more specifically SU(N) Yang-Mills theory, but include static color charges so as to obtain a description of the heavy quark potential, as in quenched approximations.

We will start by briefly describing the general theoretical setup: the Hamiltonian framework is used, where the Weyl *and* Coulomb gauge conditions, $A_0^a(\mathbf{x}) = 0$ and $\nabla \cdot \mathbf{A}^a(\mathbf{x}) = 0$, are imposed on the SU(N) gauge fields. Physical states are described by wave functionals of $\mathbf{A}^a(\mathbf{x})$ with scalar product

$$\langle \phi | \psi \rangle = \int D[\mathbf{A}] J[\mathbf{A}] \phi^*[\mathbf{A}] \psi[\mathbf{A}]. \quad (1)$$

Here, $J[\mathbf{A}]$ stands for the Faddeev-Popov (FP) determinant $J[\mathbf{A}] = \text{Det}(-\nabla \cdot \mathbf{D})$ with the spatial covariant derivative $\mathbf{D}^{ab} = \delta^{ab} \nabla + g f^{abc} \mathbf{A}^c(\mathbf{x})$. The functional integral in (1) is understood to be restricted to spatially transverse gauge fields, i.e., to those that fulfill the gauge fixing conditions.

The dynamics is defined by the Christ-Lee Hamiltonian H [1] that we do not write out. In the presence of a static color charge density $\rho_q^a(\mathbf{x})$, H contains the interaction term

$$H_q = \frac{1}{2} \int d^3x d^3y \rho_q^a(\mathbf{x}) F^{ab}(\mathbf{x}, \mathbf{y}) \rho_q^b(\mathbf{y}) \quad (2)$$

with the integral kernel

$$F^{ab}(\mathbf{x}, \mathbf{y}) = \langle \mathbf{x}, a | (-\nabla \cdot \mathbf{D})^{-1} (-\nabla^2) (-\nabla \cdot \mathbf{D})^{-1} | \mathbf{y}, b \rangle. \quad (3)$$

The vacuum expectation value $\langle F^{ab}(\mathbf{x}, \mathbf{y}) \rangle$ is called the color-Coulomb potential. It is supposed to give the dominant contribution to the confining interaction between color charges. More precisely, for large spatial distances the color-Coulomb potential provides an upper bound for the Wilson potential [2].

For the following, it will be convenient to write the FP determinant in a local form by introducing ghost fields,

$$J[\mathbf{A}] = \text{Det}(-\nabla \cdot \mathbf{D}) = \int D[\bar{c}, c] \exp \left(- \int d^3x \bar{c}^a(\mathbf{x}) (-\nabla \cdot \mathbf{D}^{ab}) c^b(\mathbf{x}) \right). \quad (4)$$

In our analysis, we will focus on the equal-time correlation functions, i.e. the vacuum expectation values of products of the field operators $\mathbf{A}^a(\mathbf{x})$ (transverse), $c^a(\mathbf{x})$ and $\bar{c}^a(\mathbf{x})$.

We can easily write down an expression for the generating functional of these correlation functions,

$$Z[\mathbf{J}, \eta, \bar{\eta}] = \int D[\bar{c}, c, \mathbf{A}] e^{-\int d^3x \bar{c}(-\nabla \cdot \mathbf{D})c} |\psi[\mathbf{A}]|^2 \times \exp \left(\int d^3x [\mathbf{J}^a(\mathbf{x}) \cdot \mathbf{A}^a(\mathbf{x}) + \bar{c}^a(\mathbf{x}) \eta^a(\mathbf{x}) + \bar{\eta}^a(\mathbf{x}) c^a(\mathbf{x})] \right), \quad (5)$$

where $\psi[\mathbf{A}]$ is the vacuum wave functional. If we formally define an “action” $S[\mathbf{A}]$ through $|\psi[\mathbf{A}]|^2 = e^{-S[\mathbf{A}]}$, (5) looks like the usual generating functional of Euclidean Green’s functions in the covariant Lagrangian formulation of the theory, only in three instead of four dimensions. Of course, $S[\mathbf{A}]$ is a complicated and a priori unknown functional of $\mathbf{A}^a(\mathbf{x})$. We will parametrize the “propagators”, the equal-time two-point correlation functions of the theory, in the most general way (restricted by symmetries) as follows:

$$\langle A_i^a(\mathbf{p}) A_j^b(-\mathbf{q}) \rangle = \frac{1}{2\omega(p)} \delta^{ab} \left(\delta_{ij} - \frac{p_i p_j}{p^2} \right) (2\pi)^3 \delta(\mathbf{p} - \mathbf{q}), \quad (6)$$

$$\langle c^a(\mathbf{p}) \bar{c}^b(-\mathbf{q}) \rangle = \langle \langle \mathbf{p}, a | (-\nabla \cdot \mathbf{D})^{-1} | \mathbf{q}, b \rangle \rangle = \frac{d(p)}{p^2} \delta^{ab} (2\pi)^3 \delta(\mathbf{p} - \mathbf{q}). \quad (7)$$

Here and in the following, we use the notation $p = |\mathbf{p}|$. The functions $\omega(p)$ and $d(p)$ will be of central interest in the rest of this contribution. Notice that the ghost propagator (7) is just the vacuum expectation value of the inverse FP operator (or rather, its integral kernel).

2 Variational principle: Dyson-Schwinger equations

A set of equations of Dyson-Schwinger type for the equal-time correlation functions of the theory was obtained in Ref. [3] from the variational principle, using a Gaussian ansatz for the vacuum wave functional. The contribution of the FP determinant was fully taken into account in [4, 5]. We write the ansatz for the vacuum functional as

$$|\psi[\mathbf{A}]|^2 = e^{-\tilde{S}[\mathbf{A}]}, \quad \tilde{S}[\mathbf{A}] = \frac{1}{2} \int \frac{d^3p}{(2\pi)^3} A_i^a(-\mathbf{p}) 2\tilde{\omega}(p) A_i^a(\mathbf{p}). \quad (8)$$

Then the variational principle with respect to the unknown function $\tilde{\omega}(p)$,

$$\frac{\delta}{\delta \tilde{\omega}(p)} \langle H \rangle = 0, \quad (9)$$

leads to a gap equation for the equal-time gluon propagator. The detailed form of the equation as well as the approximations involved in its derivation can be found in [4, 5].

The gap equation involves, apart from the gluon propagator, the ghost propagator and the color-Coulomb potential, hence further input is needed in order to arrive at a closed

system of equations. The generating functional (5) can be used to derive a Dyson-Schwinger (DS) equation for the ghost propagator in the usual way:

$$p^2 d^{-1}(p) \equiv \left(\text{---}\bullet\text{---} \right)_p^{-1} = Z_c p^2 - \text{---}\bullet\text{---}\text{---}\bullet\text{---} \quad (10)$$

In the diagrams, we represent the full equal-time ghost propagator by a dashed line and the gluon propagator by a curly line, with a dot on the lines. By extending Taylor's non-renormalization theorem [6] to the present situation, we have replaced in (10) the full ghost-gluon vertex (one of the vertices on the right-hand side) with the bare one. This replacement is also used in the gap equation.

For the color-Coulomb potential,

$$\langle F^{ab}(\mathbf{p}, -\mathbf{q}) \rangle = \langle \langle \mathbf{p}, a | (-\nabla \cdot \mathbf{D})^{-1} (-\nabla^2) (-\nabla \cdot \mathbf{D})^{-1} | \mathbf{q}, b \rangle \rangle = V_c(p) \delta^{ab} (2\pi)^3 \delta(\mathbf{p} - \mathbf{q}), \quad (11)$$

we use the following parameterization and diagrammatic representation motivated by the appearance of the inverse FP operator [cf. (7)]:

$$V_c(p) = \frac{d(p)}{p^2} p^2 f(p) \frac{d(p)}{p^2} = \text{---}\bullet\text{---}\circ\text{---}\bullet\text{---} \quad (12)$$

thereby defining the Coulomb form factor $f(p)$. Of course, the function $f(p)$ is itself unknown, and before discussing the possibility of determining it in terms of the gluon and ghost propagators in the next section, we will resort to the factorization hypothesis [7]

$$\langle (-\nabla \cdot \mathbf{D})^{-1} (-\nabla^2) (-\nabla \cdot \mathbf{D})^{-1} \rangle = \langle (-\nabla \cdot \mathbf{D})^{-1} \rangle (-\nabla^2) \langle (-\nabla \cdot \mathbf{D})^{-1} \rangle, \quad (13)$$

which is equivalent to

$$V_c(p) = \frac{d(p)}{p^2} p^2 \frac{d(p)}{p^2}, \quad (14)$$

or $f(p) = 1$. Adopting this (so far unjustified) assumption, we obtain a closed system of equations.

Before discussing the numerical solutions of the equations, we have to comment on the Gribov-Zwanziger confinement scenario [8,9]. In brief, the idea is that the existence of Gribov copies (gauge-equivalent but different transverse gauge field configurations) forces one to restrict the functional integral over the gauge field to the first Gribov region where the FP operator is positive definite.¹ By a statistical argument, in the infrared (IR) regime the dominant contribution to the functional integral comes from the region close to the Gribov

¹Actually, the first Gribov region contains Gribov copies itself, and it is necessary to further restrict the integral to the so-called fundamental modular region. It is likely that this additional complication does not affect the following argument (in the case of the Coulomb gauge).

horizon where the FP operator has zero modes. Since the ghost propagator is the vacuum expectation value of the inverse FP operator, it may be argued that the ghost propagator $d(p)/p^2$ should be more singular in the IR than p^{-2} , thus $d^{-1}(p=0)=0$, the “horizon condition” [10]. Hence, one should look for solutions that fulfill the horizon condition.

It turns out that there are two different solutions of this type [4, 11].² Both show scaling behavior in the IR, i.e., the equal-time propagators obey power laws in this kinematical regime. Furthermore, among the different contributions to the gluon propagator in the gap equation, the ghost loop diagram completely dominates the IR behavior, a property known as ghost dominance. These facts make it possible to even obtain analytical solutions for the propagators in the IR region [7, 12]. With the notations

$$\omega(p) = A p^{-\alpha}, \quad d(p) = B p^{-\beta}, \quad (15)$$

one obtains in this way a general sum rule for the IR exponents:

$$\alpha = 2\beta - 1. \quad (16)$$

Consistent solutions exist for the values $(\alpha = 0.592, \beta = 0.796)$ and $(\alpha = 1, \beta = 1)$. One may also define a running coupling constant from the ghost-gluon vertex as

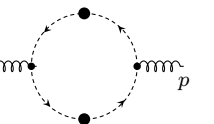
$$\alpha(p) = \frac{8}{3} \frac{g^2(p)}{4\pi}, \quad g^2(p) = g_B^2 \frac{p}{\omega(p)} d^2(p) \quad (17)$$

(g_B is the bare coupling constant). In the ultraviolet (UV), the solutions show asymptotic freedom (although not with the correct power of $\ln p$ due to the approximations to the gap equation), while $\alpha(p)$ saturates at a constant value in the IR. Analytically, one obtains $N_c \alpha(0) = 11.99$ for the solution with $\beta = 0.796$, and $N_c \alpha(0) = 16\pi/3$ for $\beta = 1$ [12].

To close this section, we comment on a possible drastic simplification of the equations: if one uses, instead of the general Gaussian ansatz (8), the lowest-order perturbative vacuum wave functional

$$|\psi[\mathbf{A}]|^2 = e^{-S_0[\mathbf{A}]} = \exp \left(-\frac{1}{2} \int \frac{d^3 p}{(2\pi)^3} A_i^a(-\mathbf{p}) 2p A_i^a(\mathbf{p}) \right) \quad (18)$$

in the generating functional (5), the complicated gap equation may be replaced by the following DS equation for the gluon propagator:

$$2\omega(p) \equiv \left(\text{diagram} \right)^{-1} = 2Z_{Ap} - \text{diagram} \quad (19)$$


²Actually, in these numerical solutions a more sophisticated approximation of the Coulomb form factor, going beyond the factorization hypothesis, was used (see below).

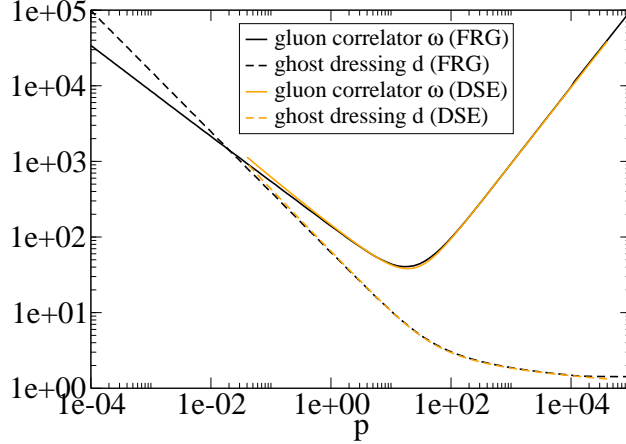


Figure 1: Comparison of the results for the propagators from the two different sets of equations [13]. The label “DSE” stands for the set that contains the gap equation and “FRG” for the set that uses (19).

In particular, (19) does not make use of the factorization hypothesis. Due to ghost dominance, the gap equation approaches (19) in the IR. Somewhat surprisingly, we have found numerically that the solutions obtained with the two different sets of equations coincide over the whole momentum range from the IR to the UV to good numerical precision (for $\beta = 0.796$) [13]. In Fig. 1, ghost and gluon propagators are represented in a double-logarithmic plot for the two different sets of equations. The slight discrepancy in the IR is due to the lower numerical precision of the earlier calculation (“DSE”) in [4].

3 Color-Coulomb potential and factorization hypothesis

The color-Coulomb potential is more directly related to physically observable quantities than the gluon and ghost propagators. For the solution with $\beta = 1$, the factorization hypothesis (14) leads to $V_c(p) \propto p^{-2-2\beta} = p^{-4}$ in the IR which corresponds to a potential in position space that rises exactly linearly for large distances. Unfortunately, the approximation used in the UV [see our remark following (17)] does not permit to relate the (Coulomb) string tension to the scale Λ_{QCD} .

We will now turn to the question of whether the factorization hypothesis is actually justified. To this end, it is convenient to represent the color-Coulomb potential with the help of a composite operator K ,

$$\begin{aligned} \langle \langle \mathbf{x}, a | (-\nabla \cdot \mathbf{D})^{-1} (-\nabla^2) (-\nabla \cdot \mathbf{D})^{-1} | \mathbf{y}, b \rangle \rangle &= \langle c^a(\mathbf{x}) K \bar{c}^b(\mathbf{y}) \rangle_{\text{GI}} , \\ K &= \int d^3 z \bar{c}^d(\mathbf{z}) (-\nabla_{\mathbf{z}}^2) c^d(\mathbf{z}) , \end{aligned} \quad (20)$$

4 The functional renormalization group

We will now turn to a different functional method, the functional (or Wilsonian) renormalization group. In order to adapt it to the case at hand, one starts with the generating functional (5) and introduces an IR cutoff k in the following way [13]:

$$Z_k[\mathbf{J}, \eta, \bar{\eta}] = \int D[\bar{c}, c, \mathbf{A}] \exp \left(- \int \frac{d^3 p}{(2\pi)^3} \bar{c}^a(-\mathbf{p}) R_k^c(p) c^a(\mathbf{p}) \right) \\ \times \exp \left(- \frac{1}{2} \int \frac{d^3 p}{(2\pi)^3} A_i^a(-\mathbf{p}) R_k^A(p) A_i^a(\mathbf{p}) \right) e^{-\int d^3 x \bar{c}(-\nabla \cdot \mathbf{D}) c} |\psi[\mathbf{A}]|^2 e^{\int d^3 x [\mathbf{J} \cdot \mathbf{A} + \bar{\eta} c + \eta \bar{c}]} . \quad (22)$$

The cutoff functions $R_k^c(p)$ and $R_k^A(p)$ have the properties

$$R_k^{c,A}(p) \rightarrow \infty \quad \text{for } p \ll k, \quad R_k^{c,A}(p) \rightarrow 0 \quad \text{for } p \gg k. \quad (23)$$

This means that the IR modes $p \ll k$ in the functional integral (22) are heavily suppressed, while in the limit $k \rightarrow 0$, $R_k^{c,A}(p) \rightarrow 0$ and $Z_k[\mathbf{J}, \eta, \bar{\eta}]$ tends toward the full generating functional $Z[\mathbf{J}, \eta, \bar{\eta}]$. In the actual calculations, we have used an exponential suppression of the IR modes,

$$R_k^c(p) = p^2 r_k(p), \quad R_k^A(p) = 2p r_k(p), \quad r_k(p) = \exp \left(\frac{k^2}{p^2} - \frac{p^2}{k^2} \right). \quad (24)$$

From (22), flow equations for the k -dependent equal-time correlation functions can be derived in the standard way [19]. They read for the propagators

$$2 \partial_k \omega_k(p) \equiv \partial_k \left[\left(\text{---} \text{---} \text{---} \right)^{-1} - R_k^A(p) \right] = \text{---} \text{---} \text{---} + \text{---} \text{---} \text{---}, \quad (25)$$

$$p^2 \partial_k d_k^{-1}(p) \equiv \partial_k \left[\left(\text{---} \text{---} \text{---} \right)^{-1} - R_k^c(p) \right] = \text{---} \text{---} \text{---} + \text{---} \text{---} \text{---}. \quad (26)$$

Here, the symbol \otimes stands for the insertion of $\partial_k R_k^{c,A}$. The non-renormalization theorem for the ghost-gluon vertex has been used in both equations. Furthermore, we have neglected diagrams that involve three- and four-gluon vertices, which is justified for the description of the IR regime if ghost dominance is assumed. Finally, we have omitted tadpole diagrams in order to be able to close the system of differential equations. Partial inclusion of the tadpole diagrams is argued in [13] to lead back to the DS equations (10) and (19) (after integrating over k).

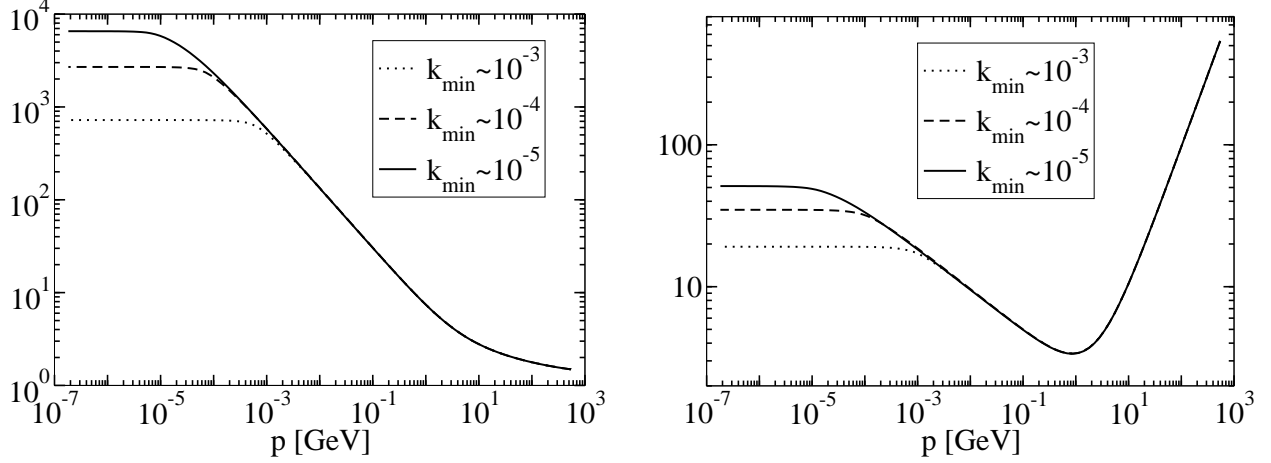


Figure 2: The results for $d(p)$ (left) and $\omega(p)$ (right) from the flow equations, for three different values of k_{\min} [13].

The general strategy is to start integrating the flow equations at a large value of k where due to asymptotic freedom the “action” $S[\mathbf{A}]$ can be replaced with $S_0[\mathbf{A}]$ from (18) and the coupling constant is small, so that the initial values of the flow are known. Then the flow equations are numerically integrated toward $k = 0$, where $\omega(p) = \omega_{k=0}(p)$ and $d(p) = d_{k=0}(p)$ are read off. Technically, it is important to convert the differential equations (25), (26) to integral equations first, so that the horizon condition and a normalization condition for $\omega(p)$ can be conveniently incorporated. The results are presented in Fig. 2, again as double-logarithmic plots. For technical reasons, the integration of the flow equations stops at a minimum value $k_{\min} > 0$. Then $\omega(p) = \omega_{k=k_{\min}}(p)$ for $p \gg k_{\min}$, and similarly for $d(p)$. From Fig. 2 it is clear that the power-law behavior of the propagators extends toward smaller momenta p as k_{\min} is lowered.

The exponents found numerically are ($\alpha = 0.28, \beta = 0.64$), smaller than for both solutions of the DS equations. They obey the sum rule (16). The fact that the exponents come out smaller than the ones from the DS equations is not entirely unexpected, since a similar behavior was found in analogous calculations in the Landau gauge [20]. Generally, the results for the exponents will slightly vary with the choice of the cutoff functions due to the approximations made in the system of flow equations. An “optimized” choice is expected to give exponents identical to the ones from the DS equations [13]. For the running coupling constant (17) one also finds saturation in the IR at a slightly smaller value than for the DS solutions.

By incorporating the composite operator K in the functional integral (22), one derives (after suitable approximations) the following flow equation for the Coulomb form factor:

$$p^2 \partial_k f_k(p) \equiv \partial_k \left(\text{diagram with wavy line and external lines} \right) = - \text{diagram 1} - \text{diagram 2} - \text{diagram 3} . \quad (27)$$

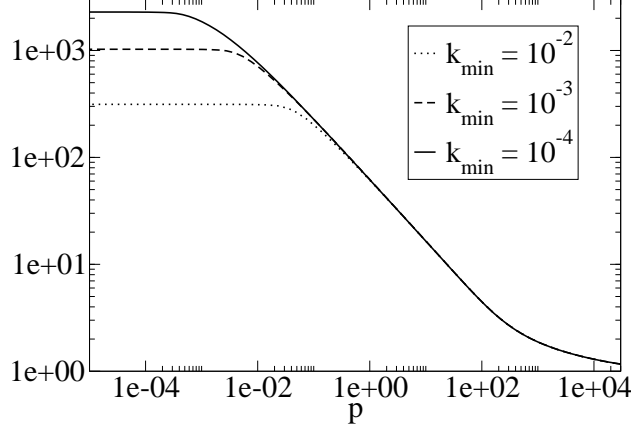


Figure 3: The Coulomb form factor $f(p)$ from (27).

Making use of the results for $\omega_k(p)$ and $d_k(p)$, this equation can be integrated. Contrary to the DS equations, (27) has a solution that is represented in Fig. 3. The IR-behavior is determined numerically to

$$f(p) \propto p^{-\gamma}, \quad \gamma = 0.57. \quad (28)$$

In particular, of course, $f(p) \neq 1$, and the factorization hypothesis is violated. With the values for the exponents from the flow equations one obtains in the IR

$$V_c(p) = \frac{d(p)}{p^2} p^2 f(p) \frac{d(p)}{p^2} = \frac{1}{p^{2+2\beta+\gamma}} = \frac{1}{p^{3.85}}, \quad (29)$$

close to $V_c(p) \propto p^{-4}$ which would correspond to a linearly rising potential in position space.

In summary, we find that functional methods are a powerful tool for the description of the nonperturbative infrared regime of nonabelian gauge theories. The formulation of these theories in the Coulomb gauge is particularly convenient, mainly because it gives direct access to the color-Coulomb potential. The Gribov-Zwanziger confinement scenario provides a conceptual framework to understand the confinement mechanism. It can be conveniently implemented via the horizon condition. In particular, we have seen that an almost linearly rising color-Coulomb potential is obtained from the functional renormalization group equations (and the factorization hypothesis is violated). It has also become clear that the approximations employed still have to be improved in order to achieve a quantitatively reliable description of the infrared region.

Acknowledgments

A.W. gratefully acknowledges support by CIC-UMSNH. M.L. and H.R. were supported by DFG-Re856/6-3.

References

- [1] Christ N H and Lee T D 1980 *Phys. Rev. D* **22** 939
- [2] Zwanziger D 1998 *Nucl. Phys. B* **518** 237
- [3] Szczepaniak A P and Swanson E S 2001 *Phys. Rev. D* **65** 025012
- [4] Feuchter C and Reinhardt H 2004 *Phys. Rev. D* **70** 105021
- [5] Reinhardt H and Feuchter C 2005 *Phys. Rev. D* **71** 105002
- [6] Taylor J C 1971 *Nucl. Phys. B* **33** 436
- [7] Zwanziger D 2004 *Phys. Rev. D* **70** 094034
- [8] Gribov V N 1978 *Nucl. Phys. B* **139** 1
- [9] Zwanziger D 1992 *Nucl. Phys. B* **378** 525
- [10] Zwanziger D 1991 *Nucl. Phys. B* **364** 127
- [11] Epple D, Reinhardt H and Schleifenbaum W 2007 *Phys. Rev. D* **75** 045011
- [12] Schleifenbaum W, Leder M and Reinhardt H 2006 *Phys. Rev. D* **73** 125019
- [13] Leder M, Pawłowski J M, Reinhardt H and Weber A 2011 *Phys. Rev. D* **83** 025010
- [14] Epple D, Reinhardt H, Schleifenbaum W and Szczepaniak A P 2008 *Phys. Rev. D* **77** 085007
- [15] Nakagawa Y *et al* 2009 *Phys. Rev. D* **79** 114504
- [16] Campagnari D, Weber A, Reinhardt H, Astorga F and Schleifenbaum W 2011 *Nucl. Phys. B* **842** 501
- [17] Burgio G, Quandt M and Reinhardt H 2009 *Phys. Rev. Lett.* **102** 032002
- [18] Voigt A, Ilgenfritz E M, Müller-Preussker M and Sternbeck A 2008 *Phys. Rev. D* **78** 014501
- [19] Wetterich C 1993 *Phys. Lett. B* **301** 90
- [20] Pawłowski J M, Litim D F, Nedelko S and von Smekal L 2004 *Phys. Rev. Lett.* **93** 152002